polymer papers

The size of phase separated regions in poly(dimethylsiloxane)/polystyrene sequential interpenetrating networks determined by small-angle neutron scattering

B. McGarey and R. W. Richards*
Department of Pure and Applied Chemistry, University of Strathclyde, Glasgow G1 1XL, UK
(Received 9 December 1985; revised 13 February 1986)

Small-angle neutron scattering has been used to investigate the size of polystyrene phase separated zones in interpenetrating networks where poly(dimethylsiloxane) was the host network. On the assumption of spherical zone morphology, the radius of the polystyrene zones has been calculated using Porod's law. The variation of this radius with polystyrene content and poly(dimethylsiloxane) crosslink density has been compared with the theoretical predictions of Yeo *et al.* Only qualitative agreement is obtained. Evidence for the existence of structure factor is presented but the scattering profiles are not well modelled by an assembly of hard spheres with a repulsive potential between the spheres. In addition to obtaining sphere radii, correlation lengths and radii of gyration of the phase separated zones have been obtained using methods which require no prior assumptions for zone morphology. Radii of gyration measurements show that the polystyrene phase separated zones have a wide distribution in size.

(Keywords: interpenetrating network; phase separated regions; small-angle neutron scattering)

INTRODUCTION

There has been considerable recent interest in the properties and phenomenology of polymer mixtures[1,2]. Much of this work has been concerned with the identification and investigation of compatible polymers which form homogenous one-phase mixtures[3,4], i.e. they are miscible at a molecular level. Contemporary with this there has been much published work on heterophase polymer mixtures amongst which are included interpenetrating polymer networks (IPN)[5-7]. In the broadest terms an IPN may be defined as the polymeric species resulting from the polymerization of a monomer whilst in intimate contact with a polymer. Generally, the polymerizing monomer and host polymer are chemically distinct and at least one of the polymers is crosslinked. If both constituents are crosslinked the resultant material is a full IPN, whereas if only one component is crosslinked it is termed a semi-IPN. Evidently there are manifold combinations of crosslinking and method of IPN synthesis and there have been a number of reviews which survey these aspects[2,6,7].

Many of the properties of heterophase polymers, particularly the mechanical properties, are thought to be determined by the morphology of the phase separated regions, i.e. their size, shape and separation and whether there is any interfacial mixing between the two phases at the boundary between guest particle and host material. Electron microscopy has been the major technique used to investigate morphological aspects of IPNs, as a result of which the factors which play a major role in determining the size of the phase separated regions (zones) have been identified. They are:

(1) Thermodynamic compatibility between the constituent polymers as quantified by the interaction parameter.
(2) Interfacial tension between guest network zones and host network.
(3) Crosslink density of component networks.
(4) IPN composition.
(5) Synthetic method utilized.

Factors (1) and (2) above are determined by the constituents of the IPN and whilst factor (5) may be varied somewhat it is only factors (3) and (4) which are in the full control of the investigator. Of these last two factors it has been found that the crosslink density of the host network has the greatest influence on the size of the phase separated regions. Theoretical predictions of the zone size, incorporating factors (1) to (4) above have been produced by Donatelli *et al.*[8] and Yeo *et al.*[9]. The equations of Donatelli *et al.*[8] are semi-empirical and have been solved for several boundary cases by Michel *et al.*[10], and whilst the equations of Yeo *et al.*[9] are on a sounder theoretical basis, they rely on the assumption that the phase separated guest zones are spherical over the whole composition range of the IPN. Nonetheless, there is good agreement between theory and measurements made by transmission electron microscopy. Data from dynamic mechanical analysis contradict these results since the data

* To whom correspondence should be addressed.
Present address: Polymer Science and Engineering, Graduate Research Center, Room 701, University of Massachusetts at Amherst, Amherst, MA 01003, USA

0032-3861/86/091315$03.00

indicates that co-continuity exists between the two constituent networks of the IPN[11]. Further evidence in support of network co-continuity has been obtained by Widmaier and Sperling[12] using a decrosslinkable guest polymer network.

The structure of condensed matter may also be investigated by small-angle scattering of X-rays (SAXS) or neutrons (SANS), these techniques have the advantage of using specimens considerably thicker than those used in transmission electron microscopy, consequently the data obtained is more characteristic of the *average* structure. Application of small-angle techniques to the evaluation of IPN structure has been limited. Small-angle X-ray scattering has been used by Lipatov *et al.*[13,14] on polyurethane/polyurethane acrylate IPNs whilst Blundell *et al.*[15] have investigated polyurethane–poly(methyl methacrylate) IPNs; lastly Sperling has made reference to results obtained by SANS on a polystyrene in polybutadiene IPN[2].

We report here the results of a SANS investigation of a deuteropolystyrene (PSD) in poly(dimethylsiloxane) (PDMS) sequential IPN. The objectives were severalfold; to determine the size of the phase separated PSD zones and an estimate of the breadth in the size distribution, assess any evidence for the existence of a diffuse interfacial layer at the boundary of the PSD zones and lastly, to ascertain if there was a preferred separation distance between the PSD zones. A summary of the theory of phase separated zone size in IPNs is given below together with salient theory for the interpretation of small-angle scattering data.

THEORY

Size of phase separated regions in IPNs

A summary of the theory due to Yeo *et al.*[9] is presented, together with the equation derived by them which is pertinent to the sequential IPNs investigated here. The theory rests on four assumptions: (1) thermodynamic equilibrium exists during the whole process of heterophase IPN formation; (2) the phase separated regions of the guest network are monodisperse and have a spherical shape; (3) the network chains obey Gaussian statistics; (4) a sharp interface exists between the two constituents of the IPN. Schematically, the process of IPN formation is modelled by three distinct stages to facilitate the calculation of the individual contributions to the overall free energy change of IPN formation. The host network is swollen by the guest monomer and crosslinker; the guest monomer is polymerized to form a hypothetical compatible, homogenous mixture of the two networks; the guest network then phase separates to form a spherical region of pure guest polymer network. The major contribution to the free energy change arises from the last stage and involves calculation of the entropy changes consequent on the deformation of each network and the interfacial free energy change on formation of a phase separated spherical region. For the case of sequential IPNs wherein both constituents are crosslinked, it is presumed that the molecular weights are infinite and the diameter of the guest polymer network regions is given by:

$$D_2 = 4\gamma_{12}[RT(AV_1 + BV_2)]^{-1} \quad (1)$$

where D_2 = phase separated region diameter;
γ_{12} = interfacial tension between the two polymers;
V_1, V_2 = crosslink densities of host (1) and guest (2) networks respectively;
$A = (0.5\phi_2)(3\phi_1^{1/3} - 3\phi_1^{4/3} - \phi_1 \ln\phi_1)$;
$B = 0.5(\ln\phi - 3\phi_2^{2/3} + 3)$;
ϕ_1, ϕ_2 = volume fractions of the host and guest polymers respectively.

Since the constant A in equation (1) is between 5 to 10 times greater than B, then the crosslink density of the host network is much more effective in determining the size of the guest polymer network; additionally it is evident that the interfacial tension also plays an important role in determining the zone diameter, D_2. *Figure 1* shows the radius of polystyrene zones in PDMS for three different crosslink densities of PDMS calculated from equation (1) using a value of 6.1 dyne cm^{-1} for γ_{12}.[16] We note that apart from dramatically influencing the magnitude of the radius, the crosslink density also changes the curvature of the dependence. Such large changes in R are not observed when the crosslink density of the guest network is altered (*Figure 2*), furthermore a very large increase in guest network crosslink density is needed to change the radius of the polystyrene zones.

Small-angle scattering from particulate assemblies

Small-angle scattering measurements entail the observation of the intensity of scattering from a specimen

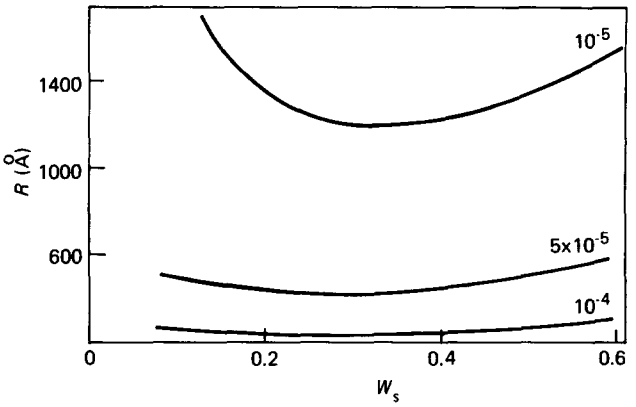

Figure 1 Influence of PDMS network crosslink density on polystyrene zone radius calculated from equation (1). Crosslink density of polystyrene = 1×10^{-4} mol ml^{-1}, PDMS crosslink density marked on curves

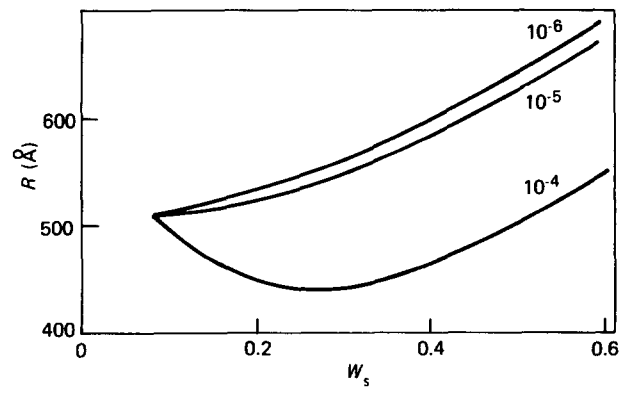

Figure 2 Influence of polystyrene guest network crosslink density on zone radius calculated from equation (1). PDMS crosslink density = 5×10^{-5} mol ml^{-1}, polystyrene crosslink density marked on curves

as a function of the scattering vector, Q, where $Q=(4\pi/\lambda)\sin\theta$, λ is the radiation wavelength and 2θ the scattering angle. The scattering arises from fluctuations in density of the material, for SAXS, fluctuations in electron density are responsible for scattering whilst SANS is caused by scattering length density fluctuations. The foundations of small-angle scattering are dealt with in a number of publications[17-21].

The theoretical form of variation of scattered intensity, $I(Q)$ as a function of scattering vector, Q, was obtained for spherically symmetric monodisperse particles by Zernicke and Prins[22] as

$$I(Q)=CK_fNP(Q)S(Q) \tag{2}$$

where C = instrumental constant;
K_f = contrast factor;
N = number of scattering particles;
$P(Q)$ = single particle form factor;
$S(Q)$ = structure factor for the particulate assembly.

The single particle form factor, $P(Q)$, is determind by the particle morphology and its characteristic dimension. For spherical particles the characteristic dimension is the radius, R, and we have[17]

$$P(Q)=V_p^2[9\pi/2(QR)^3]J_{3/2}^2(QR) \tag{3}$$

where V_p = particle volume
$J_{3/2}(X)$ = Bessel function of order 3/2 with argument X.

The contrast factor, K_f, for neutron scattering is given by $(\rho_p-\rho_m)^2$, where ρ_p and ρ_m are the coherent scattering length densities of the particle and the matrix in which it is embedded. These two parameters are calculable from literature data[21].

The structure factor, $S(Q)$, encompasses the possibility that interference effects may occur between radiation scattered from different particles which may be regularly arranged to some degree. Various forms of the structure factor have been derived and they may be considerably simplified where organizational regularity is of a high degree as in block copolymers. The most general form for $S(Q)$ is[23]:

$$S(Q)=1+4\pi\rho_n\int_0^\infty (g(r)-1)[\sin(Qr)/(Qr)]r^2\mathrm{d}r \tag{4}$$

where $g(r)$ is the pair distribution function characteristic of the particle arrangement and ρ_n the particle number density. A number of attempts at solving equation (4) have been made, all of them treating the particles as hard spheres; amongst the solutions are those of Debye[24] and Fournet[25]. However, the most generally useful, since it accounts for interactions between all particles in the scattering volume, is the structure factor obtained by Ashcroft and Lekner[26] from the hard sphere model of liquids proposed by Percus and Yevick[27]. The structure factor obtained is dependent not only on the value of Q but also the volume fraction and radius of the hard sphere particles.

$$S(Q,R,\phi)=1/(1+24\phi G(A)/A) \tag{5}$$

where $A=2QR$
ϕ = sphere volume fraction
$G(A)=(\alpha/A^2)(\sin A-A\cos A)+(\beta/A^3)(2A\sin A+(2-A^2)\cos A-2)+(\gamma/A^5)(-A^4\cos A+4[(3A^2-6)\cos A+(A^3-6A)\sin A+6])$
$\alpha=(1+2\phi)^2/(1-\phi)^4$
$\beta=-6\phi(1+\phi/2)^2/(1-\phi)^4$
$\gamma=(\phi/2)(1+2\phi)^2/(1-\phi)^4$

Owing to the form of $S(Q)$ there is always a region of Q where $S(Q)$ obtains an asymptotic value of 1, in this region the scattered intensity is determined by the isolated particle and the dimensions of the particle may be obtained. However, the structure factor is *always* modulated by $P(Q)$ no matter what Q range is utilized.

The form of $P(Q)$ will be greatly influenced by polydispersity of sphere size and modest distributions have been shown to produce a severe loss of resolution of the maxima but without significant reduction in the average scattered intensity[28,29]. It has been shown by van Beurten and Vrij[30] that the structure factor is less influenced by particle size polydispersity being negligible for distributions with standard deviations *ca.* 10% or less. However, for wider particle size distributions the maximum in the structure factor is reduced in amplitude and shifted to lower Q, these effects becoming more apparent with increasing distribution width.

The above description relies on the scattering particles having a well defined geometry, however it may be the case that the scattering particle geometry is ill defined and cannot be so treated. In such cases a statistical description is more useful and the best known of these is the use of the correlation function pioneered by Debye and Bueche[31], and subsequently expanded on by Debye, Anderson and Brumberger[32]. In this description for an isotropic assembly of scattering particles then

$$I(Q)=K\langle\eta^2\rangle\int_0^\infty \gamma(r)(\sin(Qr)/(Qr))\mathrm{d}r \tag{6}$$

where $\langle\eta^2\rangle$ is the average value of the square of the density fluctuations in the system and is equivalent to K_f for SANS.

The correlation function, r, of the particulate assembly takes values between one at $r=0$ and zero at $r=\infty$. For a randomly oriented assembly of particles with a sharp interface between particle and matrix then the correlation function can be approximated by an exponential function:

$$\gamma(r)=\exp(-r/a_c) \tag{7}$$

and in this case

$$I(Q)=C/(1+a_c^2Q^2)^2 \tag{8}$$

where C is a collection of constants including the contrast factor and a_c is the correlation length of the scattering particles. The mean chord length in each of the phases can then be obtained from the Porod relationships[33].

$$l_1=a_c/\phi_2 \quad \text{and} \quad l_2=a_c/\phi_1$$

where ϕ_1 and ϕ_2 are the volume fractions of the two phases. The chord length is the average length through the

phases of lines drawn at random through the scattering system.

EXPERIMENTAL

Materials

Poly(dimethylsiloxane) networks of differing crosslink density were prepared from gums generously donated by J-Sil Silicones Ltd, Worsley, Manchester. The characteristics of these gums, which contained different amounts of vinyl end groups, are given in *Table 1*. The number-average molecular weights were determined by membrane osmometry whilst low-angle laser light scattering was used to measure the weight-average molecular weight. Each gum contained 1% (w/w) dicumyl peroxide and networks were prepared by compression moulding gum samples at 170°C for 10 min followed by a post cure treatment of 4 h at 200°C in a ventilated oven. Networks obtained by this procedure were transparent discs 10 cm in diameter and approximately 1 mm thick.

Perdeutero styrene (98 atom%), obtained from Aldrich, was washed with a 10% aqueous solution of sodium hydroxide followed by a water wash and finally dried over calcium chloride. Owing to the small amount available it was not distilled after drying.

Preparation of polyperdeuterostyrene–poly(dimethylsiloxane) interpenetrating-networks

Previous work had established a swelling *versus* time curve for PDMS networks immersed in hydrogenous styrene. Small PDMS network discs (*ca.* 1.5 cm in diameter) were cut from the larger networks described above, these were then swollen in perdeuterostyrene monomer containing 0.5% (w/w) AIBN as initiator and 1% divinylbenzene[34] as crosslinker. Networks were removed from this solution at differing times depending on the desired final composition of the IPN, the surfaces were blotted dry and the swollen networks placed in a close fitting mould lined with PTFE and left there for 12 h to obtain uniform monomer distribution. After this time the moulds were heated to 80°C for 3 h. The IPNs were then removed from the mould and dried under vacuum for one week. The weight fraction of polyperdeuterostyrene in the IPNs prepared in this way varied from 0.1 to 0.6, all were white, opaque materials which were rubbery at low PSD content and hard materials at high PSD content.

Table 1 Characteristics of poly(dimethylsiloxane) precursor polymers and the crosslink densities of the networks obtained

Code	Description	M_n (10^5 g mol^{-1})	M_w (10^5 g mol^{-1})	V_1 (10^{-5} mol ml^{-1})
PDMS 1	25% content of 0.05 mol% vinyl end stopped PDMS	3.22	6.42	2.49
PDMS 2	0.05 mol% vinyl end stopped PDMS	2.67	4.78	4.55
PDMS 3	0.02 mol% pendant vinyl groups in PDMS molecules	2.13	5.55	6.6

Determination of crosslink density of PDMS networks

The crosslink density of each PDMS network used was determined by two methods. Firstly, from the equilibrium swelling in toluene, using the values of the interaction parameter interpolated from data quoted by Orwoll[35] and substituting values into the classical Flory–Rehner[36] equation. Secondly, using the shear modulus calculated from stress–strain measurements on the PDMS networks. The values of crosslink density obtained from the two methods were in reasonable agreement with each other and the mean values are reported in *Table 1*.

Small-angle neutron scattering

SANS measurements on the IPNs were made at the Institut Laue-Langevin, Grenoble, France, using the D11 and D17 diffractometers. The range of scattering vector covered was $2\times10^{-3}\ Q/\text{Å}^{-1}\times0.35$. The scattered intensity from each IPN was normalized to the scattering from distilled water with a path length of 1 mm. After normalization, the 'excess' scattering due to the PSD zones in the IPN was obtained by subtracting the scattering of the pure PDMS networks, due account being made for any differences in neutron transmission between IPN and PDMS network. Data correction and normalization was performed at the Institut Laue-Langevin using the software suite written by Dr R. E. Ghosh[37].

RESULTS AND DISCUSSION

A typical scattering profile obtained for the IPNs investigated here is shown in *Figure 3*. Although there appears to be some evidence for a shoulder at very low Q, the chief characteristic is the featureless attenuation of scattered intensity with increasing Q. For $Q>0.12$ Å^{-1}, the scattering intensity has an asymptotic value, the magnitude increasing as the amount of PSD in the IPN increases. We have interpreted this asymptotic intensity as the incoherent scattering of the PSD and it has been subtracted from the data to yield scattering profiles as shown in *Figure 6*. A double logarithmic plot of intensity as a function of Q as shown in *Figure 4* also indicates a maximum $Q\approx2.5\times10^{-3}$ Å^{-1}; this identification of a maximum can only be tentative since it appears at the extreme of the range of Q we have investigated. *Figure 4* is, however, noteworthy for the monotonic decrease in intensity over the range $0.01\leqslant Q/\text{Å}^{-1}\leqslant0.1$. A linear least

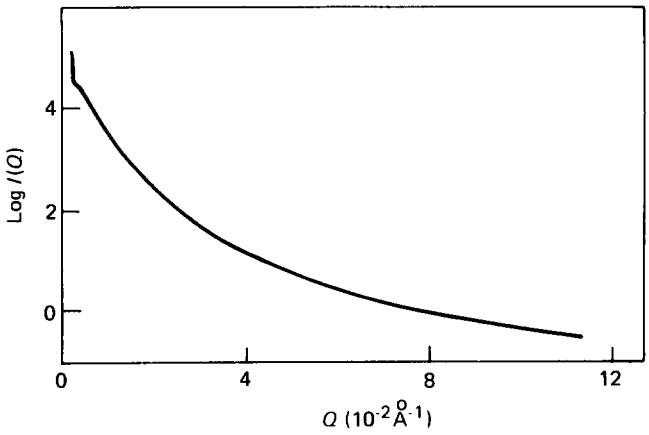

Figure 3 Scattered intensity obtained by SANS for an IPN prepared from PDMS 3, with a PSD weight fraction of 0.6

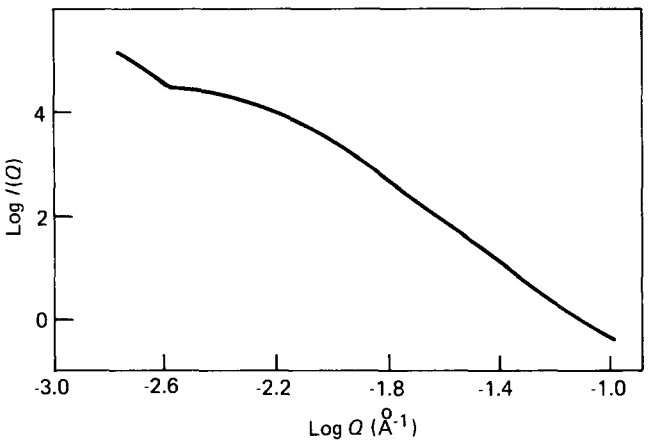

Figure 4 Log–log plot of the data in *Figure 6*

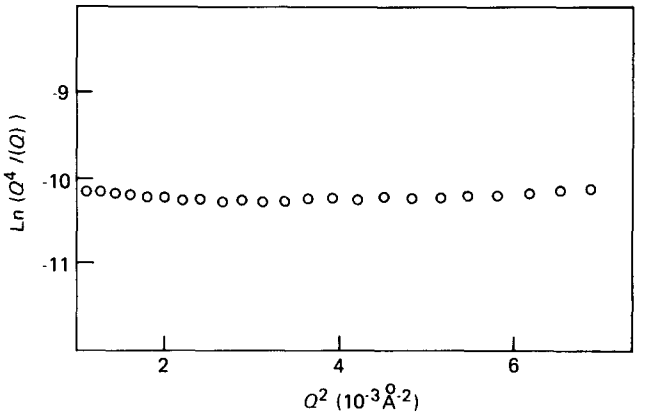

Figure 5 Typical plots of $Q^4 I(Q)$ vs. Q for an IPN with PSD weight fraction of 0.6. Note the constancy of $Q^4 I(Q)$ over the wide range of Q

mean squares analysis on the data in this region yields the relation

$$I(Q) \propto Q^{-4.1 \pm 0.2} \tag{9}$$

The scattering described by equation (9) is the classical Porod type scattering[38] and enables us to calculate the size of the PSD zones in the IPN.

Porod law analysis of scattering data

Porod showed that for randomly oriented particles with sharp boundaries, i.e. no diffuse layer at the surface, and for a region of Q wherein Q (smallest characteristic dimension of the particle)$^{-1}$ the scattering is given by

$$I(Q) = K 2\pi (A_p/V_p^2) Q^{-4} \tag{10}$$

where K is a collection of factors (*vide infra*), A_p the surface area of the particles whose volume is V_p.

We have noted above that this law is followed for the PDMS/PSD IPNs investigated here, consequently there is no diffuse interfactial layer[39] at the PSD zone boundaries where mixing of PSD and PDMS may have taken place. We have not therefore analysed the data further to determine an interfacial layer thickness. From equation (10) we note that the product $Q^4 I(Q)$ should be a constant value, and *Figure 5* shows this to be true except at very high Q. The increase of $Q^4 I(Q)$ in this range of Q is attributed to density fluctuation *within* the PSD zones and possibly some parasitic scattering. If we assume, in common with Yeo *et al.*, that the PSD zones are spherical, then the ratio (A_p/V_p) in equation (10) is $3/R$ where R is the spherical PSD zone radius. Earlier work[39] has evaluated the factor K in equation (10) hence we have

$$Q^4 I(Q) = 4\pi D_s T_s K_f \phi_p V_p 3/V_p R(1 - T_w)$$
$$= 12\pi D_s T_s K_f \phi_p/(1 - T_w) R \tag{11}$$

where D_s is the IPN thickness, T_s the neutron transmission factor for the IPN (i.e. ratio of transmitted beam intensity to incident beam intensity), T_w the neutron transmission factor for the water specimen used as a calibrant in the neutron scattering measurements and ϕ_p the volume fraction of PSD in the IPN. The radii of the PSD zones (assumed to be spherical) calculated using equation (11) are given in *Table 2* and plotted as a function of PSD weight fraction in *Figure 6*.

These data do not display the large influence of PDMS crosslink density expected from equation (1) and discussed earlier, the radii are all of the same order of magnitude and all have a large increase for styrene weight fractions greater than 0.4. Included in *Figure 6* are the theoretical curves calculated from equation (1). For this

Table 2 Dimensions of PSD zones obtained from neutron scattering data

Weight fraction of PSD	Radius (Å) (Porod law)	Correlation length (Å) (Debye plot)	Chord length (Å)
A PDMS 1			
0.54	571	205±10	446
0.47	197	157±5	296
0.37	169	152±5	287
0.25	163	152±5	203
0.16	202	175±8	208
B PDMS 2			
0.64	584	153±5	425
0.49	217	151±5	296
0.32	153	139±4	204
0.16	161	161±6	192
C PDMS 3			
0.6	535	196±8	490
0.45	336	171±8	310
0.38	193	158±5	255
0.28	156	157±5	218
0.20	243	178±6	223

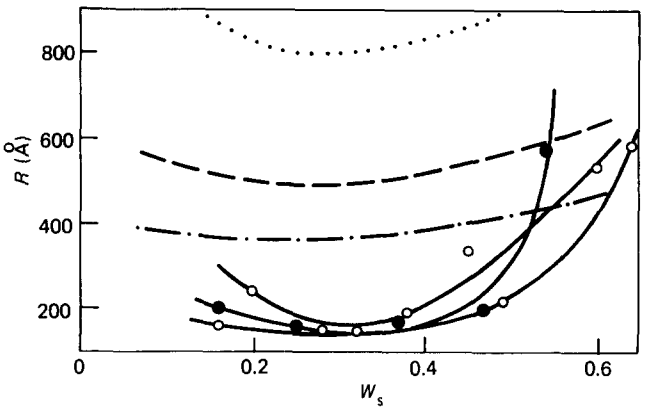

Figure 6 Radius of PSD zones obtained from Porod law analysis as a function of PSD weight fraction. Full lines are drawn as a guide to the eye. (○) PDMS 3; (◑) PDMS 2; (●) PDMS 1. Theoretical curves calculated from equation (1):
(·····) PDMS 1; (– – –) PDMS 2; (–·–·–) PDMS 3

purpose the crosslink density V_2 of the PSD regions was obtained from the swelling in toluene of a sample of crosslinked polystyrene prepared under the same conditions used for IPN preparations, i.e. identical initiator and crosslinking agent concentrations and temperature of polymerization, the crosslink density of this polystyrene was 7.7×10^{-5} mol ml^{-1}. There are features of theoretical and experimental curves which are in agreement, notably the minimum in the radius at a PSD weight fraction of *ca.* 0.3. However the experimental data is considerably more curved and much smaller in magnitude than the theoretical predictions. In equation (1), it is the interfacial tension, γ_{12}, which has the greatest uncertainty. To our knowledge there is only one value quoted in the literature[16], for this polymer combination, calculation of γ_{12} leads to somewhat equivocal results. Calculation using the geometric mean[40] of the surface tensions of the individual polymers leads to a value of 8.8 dyne cm^{-1} whilst use of the mean field theory of Helfand and Sapse[41] yields a value of zero. Notwithstanding any flexibility in the value of γ_{12}, it cannot be the sole source for the disparity between experiment and theory since the influence of PDMS crosslink density is negligible. It appears that the crosslink density of the PDMS in the region of the PSD zones is higher than the value obtained for the pure PDMS network since, as we have seen, it is this factor which influences the size of the PSD zones to the greatest extent. Increased crosslinking could be envisaged due to diffusion of the divinyl benzene crosslinking agent out of the PSD zones into the neighbouring PDMS. However, comparative swelling measurements show that the divinyl benzene is preferentially absorbed by the polystyrene regions, consequently it is unlikely that a substantial increase in the local crosslink density of the PDMS takes place due to this mechanism.

The curvature of the experimental data is significantly greater than theoretical predictions, at the higher weight fractions of PSD. This rapid increase in radius may be an indication of co-continuity of PSD and PDMS networks, but electron microscopy on these IPNs reveals no firm evidence for this[42]. Aggregation of several individual PSD zones could be another cause of the increase in radius and this would lead to a distribution in PSD zone sizes.

Hosemann analysis of scattering data

Notwithstanding the questionable validity of assuming the PSD zones to be spherical, the absence of any distinct maxima in *Figure 6* at intermediate Q values clearly shows they are not monodisperse. Therefore, PSD zone size may be better discussed in terms of a radius of gyration, R_g, and a distribution function for R_g. This may be achieved by utilizing the analytical procedures of Hosemann[43] which were generalized to R_g by Guinier and Fournet[17]. The analysis consists of plotting the data as in *Figure 7* and identifying the values of Q where the data has a maximum (Q_m) and where the tangent to the point of inflection intersects the Q axis (Q_t). Hosemann gives the equation for the arithmetic mean of R_g as:

$$R_g^m = t_0 \Gamma(n/2+1)/\Gamma(n/2+1/2) \qquad (12)$$

where $r_0 = (6/(n/2))^{1/2}/Q_m$ and the value of n is obtainable from

$$(Q_t/2Q_m) - 1 = (2(n+1))^{-1/2} \qquad (13)$$

Values of Q_t and Q_m were obtained by numerical analysis of data plotted as in *Figure 7*. In brief this consisted of fitting the data by a Chebyshev polynomial the degree of which was chosen to give the best fit to the data. This Chebyshev polynomial was then approximated by a power series which could be differentiated to identify turning points and points of inflection as the roots of the first and second differentials respectively. All these computations were made on the VAX 11/782 computer located in the University and utilizing NAG and Harwell subroutine libraries. *Table 3* reports the values of n, r_0 and R_g^m so obtained for the PDMS/PSD IPNs studied here, however as *Figure 8* shows there appears to be no systematic correlation between R_g^m, and network crosslink density or composition. The values of n obtained indicate a very broad distribution of PSD zone size since the fractional standard deviation varies between 0.43 and 0.57, the form of the Maxwellian distribution is shown in *Figure 9* for one of the IPNs investigated.

Correlation length analysis of scattering data

Whilst the Hosemann analysis may be more applicable than the assumption of a spherical geometry for the PSD zones, it still necessitates the assumption of a particular form of the distribution in particle size. A more useful analysis may therefore be the Debye correlation length analysis especially in view of the speculations of Sperling[2] which views the phase separated zones as regions of ill

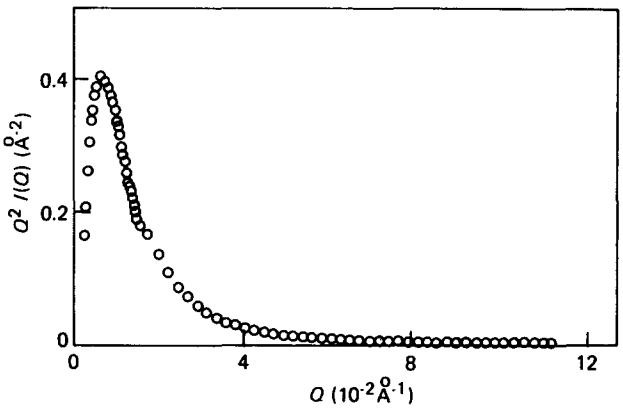

Figure 7 Typical Hosemann plot for an IPN prepared from PDMS 3 with PSD weight fraction of 0.38

Table 3 Results of Hosemann analysis of SANS data for IPNs

Weight fraction of PDMS	n	r_0 (Å)	R_g^m (Å)
A PDMS 1 network			
0.54	1.26	251	315
0.47	1.66	192	318
0.37	1.28	193	247
0.25	1.54	193	296
0.16	1.23	229	282
B PDMS 2 network			
0.64	0.70	222	156
0.49	0.86	214	184
0.32	0.54	204	109
0.16	0.85	230	194
C PDMS 3 network			
0.6	1.04	259	269
0.45	1.18	221	261
0.38	1.42	196	279
0.28	1.18	205	241
0.20	1.17	235	274

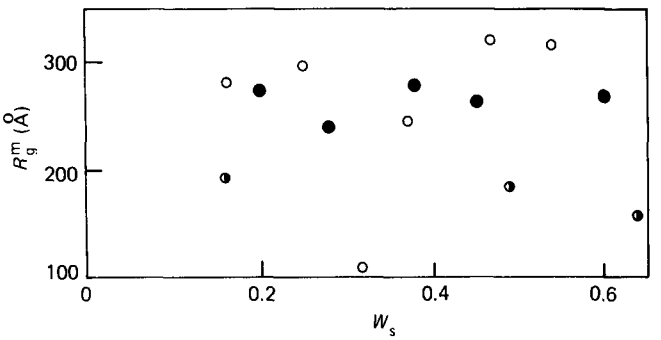

Figure 8 Radii of gyration of PSD zones calculated from Hosemann plots: (○) PDMS 3; (◑) PDMS 2; (●) PDMS 1

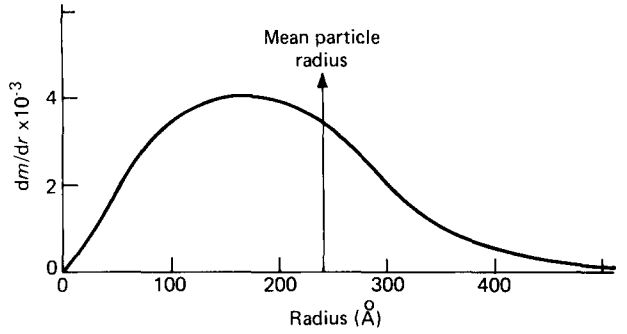

Figure 9 Maxwellian distribution obtained from the parameters of the Hosemann analysis for the IPN containing a PSD weight fraction of 0.28 in PDMS 3

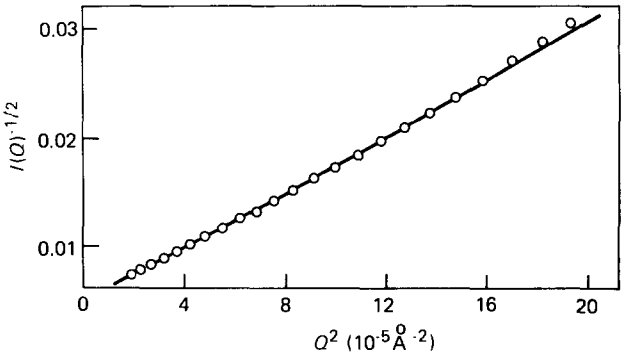

Figure 10 Typical Debye plot. IPN prepared from PDMS 3 with PSD weight fraction of 0.45

defined shape with irregular edges. A representative plot of the data plotted according to equation (8) is shown in *Figure 10*, and gives an excellent straight line. Correlation lengths were calculated from the slope and intercept of linear least squares fits to the data, the values obtained are given in *Table 2* together with the mean chord length through the PSD phase of the IPN. As *Figure 11* shows, the variation of correlation length with composition goes through a distinct minimum and whilst the values for each of the PDMS networks are separate from each other, they do not have the correlation with crosslink density expected from the theory of Yeo *et al.*[9]. The distinction between each PDMS network all but disappears when the chord length is plotted as a function of PSD weight fraction (*Figure 12*). For PSD weight fractions < 0.4 the chord lengths are essentially the same for all three PDMS crosslink densities. At higher weight fractions, the data points do diverge from each other, but not in the manner expected from theory. The absence of any effect of PDMS crosslink density again suggests the occurrence of additional crosslinking in the immediate neighbourhood of the PSD zones whilst the increase in chord length for PSD weight fractions greater than 0.5 may indicate the presence of network co-continuity.

Interparticle separation

It was remarked earlier that there was some evidence for a maximum in the scattered intensity at very low Q and this implies the existence of a preferred separation distance. In view of the excellent fit of the data over the Q range 4×10^{-3} Å to 0.014 Å^{-1} to the Debye equation (equation (8)), then any preferred separation distance has to be incorporated into a random assembly of the polystyrene zones. Such random assemblies of scattering particles are encountered in concentrated colloidal dispersions and the small-angle scattering from them has been analysed with the aid of Percus–Yevick theory[43–46]. The procedure by which the structure factor, $S(Q)$, is obtained is by the division of the scattering for the concentrated dispersion by the scattered intensity for an individual particle, i.e. $P(Q)$[46]. For colloidal dispersions $P(Q)$ can be obtained unambiguously from measurements on dilute dispersions. This method is not available to us here, additionally, for IPNs we have to make an assumption regarding the morphology of the PSD zones. Therefore we have adopted a variant of the procedure referred to above for colloidal dispersions. Firstly, we have assumed the PSD zones to be spherical with radii determined by the Porod law analysis. Secondly, we have assumed that in range $3 \times 10^{-2} \leqslant Q/\text{Å}^{-1} \leqslant 0.1$ the value of $S(Q)$ is unity, this assumption is not drastic in view of the

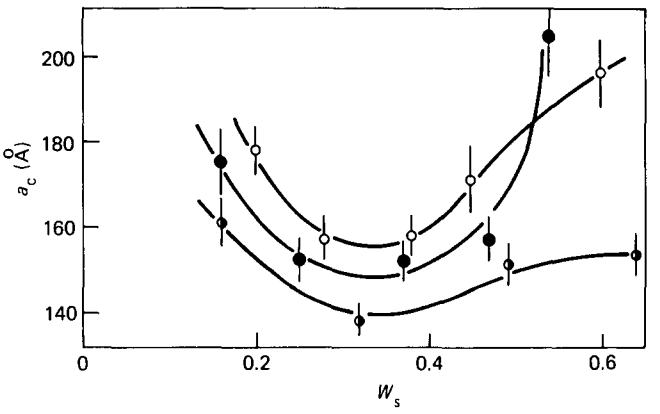

Figure 11 Correlation lengths obtained from least squares analysis of Debye plots. Lines through data are guides to the eye: (○) PDMS 3; (◑) PDMS 2; (●) PDMS 1

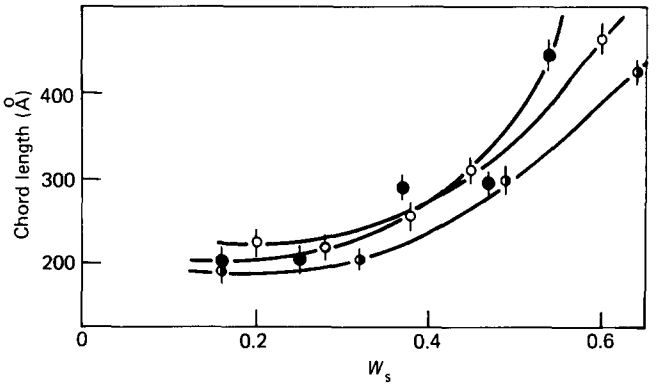

Figure 12 Chord length through the PSD zones as a function of PSD weight fraction. Lines are guides to the eye. Symbols as in *Figure 11*

evident wide distribution in PSD zone radii. The scattering law for a sphere with a Gaussian size distribution has been fitted to the scattering data in the range $3 \times 10^{-2} \leqslant Q/\text{Å}^{-1} \leqslant 0.1$, the standard deviation of the distribution being an adjustable parameter of the fit together with a multiplying factor to obtain coincidence in the magnitude of experimental data and the calculated scattering curve. The scattering law for the spherical PSD zone was then calculated over the whole range of Q and investigated using the parameters obtained by this fitting process. Typically, best fits were obtained for a fractional standard deviation of 0.15, larger standard deviations did not produce data with the required attenuation of intensity with Q. The experimental scattered intensity data were then divided by this calculated single particle scattering law to obtain the form of $S(Q)$ for the PSD zones in the IPNs. *Figure 13* shows the results of this process for two IPNs with PDMS3 as the host network. The features in these two diagrams are common to the results obtained for all the other IPNs, i.e. at PSD weight fractions greater than 0.4 a distinct first maximum is noted with a rather ill-defined second maximum. At lower PSD weight fractions there appears to be a maximum at much lower Q. It should be noted that these maxima are observed in a region of Q where $P(Q)$ is a smoothly increasing curve (*Figure 14*) and consequently do not arise from minima in $P(Q)$. The indication of a maximum at very much lower Q for the IPN with the lower content of PSD is in qualitative agreement with expectations if the PSD zones exist as discreet zones uniformly distributed throughout the PDMS network. The total scattering from an assembly of spheres has been calculated using the Percus–Yevick type approximation discussed earlier. Comparison with the experimental data (*Figure 15*) shows poor agreement in the low Q range. The maximum in the theoretical scattering appears at a much higher Q than is evident in our data and additionally there is a second maximum arising from $P(Q)$ which does not appear in the experimental data. It could be postulated that the effective

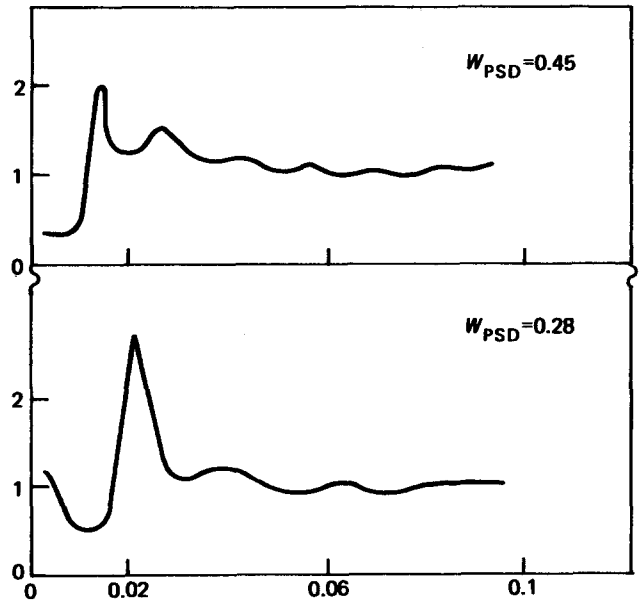

Figure 13 Structure factors obtained from two IPNs with PDMS 3 as host network, PSD weight fractions as noted on plots. Curves obtained by the division of experimental data by calculated $P(Q)$ obtained from fitting at high Q values

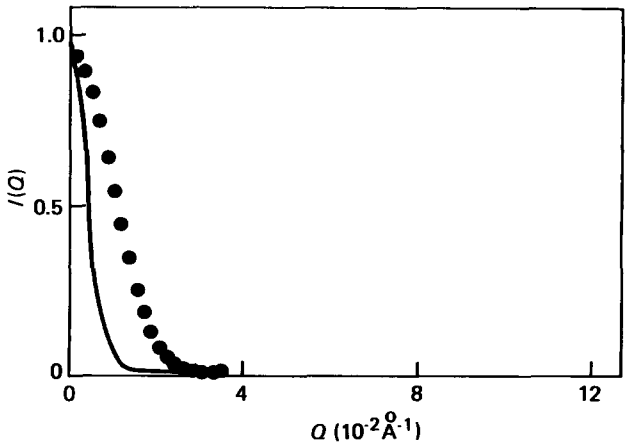

Figure 14 Forms of $P(Q)$ used to obtain the structure factors in *Figure 13*. (———) $P(Q)$ for PSD zones in IPN with $W_s = 0.45$; (·····) $P(Q)$ for PSD zones in IPN with $W_s = 0.28$

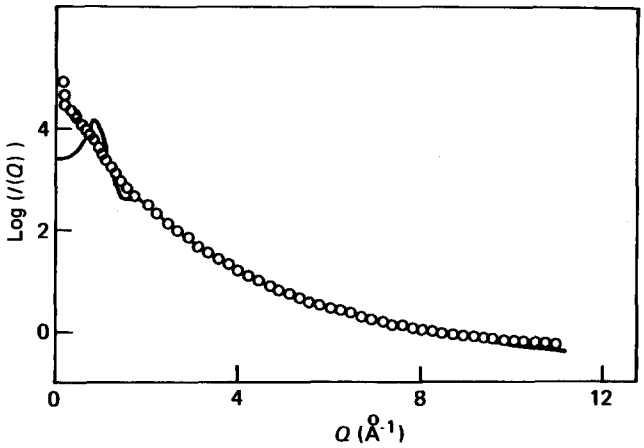

Figure 15 Comparison of calculated scattering from assembly of spheres with experimental data for an IPN with a PSD weight fraction of 0.45 in PDMS 3. Parameters of model; sphere radius = 336 Å, per cent standard deviation = 15%; volume fraction = 0.45: (○) experimental data; (– – –) calculated scattering

PSD sphere size and volume fraction are actually greater than the measured values due to the apparent increase in crosslink density of the PDMS in the immediate neighbourhood of the PSD zones, i.e. there is a layer of immobility associated with each PSD zone. This idea has been used by Kinning and Thomas[47] in discussing the scattering from block copolymers, however its application here produces no better agreement between theory and data, since the only effect is to increase the amplitude of the maximum at low Q. A possible source of the disagreement between theory and experimental data could be the very broad distribution of PSD zone size which the Hosemann analysis indicates. Such a wide distribution in particle size has not been incorporated into the calculations for $S(Q)$ in *Figure 15*, and whilst theory does suggest that the maximum of $S(Q)$ is shifted to lower Q in the presence of broad particle distributions it should also be noted that the oscillations at higher Q disappear for such broad distributions. Evidently, a more detailed analysis for the existence of a structure factor in these IPNs must await the collection of scattering data at much lower Q whereby any maxima present may be resolved.

Comparison with other IPNs

Blundell *et al.*[15] have reported the results of a SAXS investigation of a simultaneous IPN with poly(methyl methacrylate) as guest polymer in a polyurethane network. Their data were interpreted via Debye plots and reported as chord lengths in the methacrylate phase and agreed well with electron microscopy results. The chord lengths obtained for this system were very large, ranging from 770 Å to 3600 Å; the influence of crosslink density was not investigated in detail, however it is noteworthy that the dependence of the chord length on methacrylate content has a curved form very similar to that in *Figure 15*. Shilov *et al.*[13] also used SAXS to investigate polyurethane–polyurethane acrylate simultaneous IPNs. The analysis of their data produced interfacial diffuse boundary layer thicknesses of between 40 Å and 20 Å, not surprising in view of the similarity of the two components of the IPN. Correlation lengths and equivalent spherical radii were obtained and values varied between 120 Å to 750 Å in a manner which did not, apparently, depend on the IPN composition. For a polyurethane–polystyrene IPN[14], they report correlation lengths varying from 320 Å to *ca.* 200 Å for compositions ranging from weight fractions of 0.04 to 0.35 of the guest polymer. Sperling[2] reports chord lengths for polybutadiene regions in IPNs and semi-IPNs with polystyrene, the values being between 49 Å and 131 Å, however the polybutadiene weight fraction only varied between 0.19 and 0.27 and it was not made clear which were the full IPNs.

The values of the length parameters for the PSD zones we have obtained here are of the same order of magnitude as the majority of those discussed above, notwithstanding the variety of materials used and the synthetic methods employed. Only the data of Blundell *et al.*[15] is in major disagreement with other data, however the internal consistency of their data suggests that this discrepancy with other data is not an artefact. In an earlier paper[48], they gave the results of an investigation into the influence of crosslink density of the polyurethane on the methacrylate zone size. For these networks which had been allowed to cure for longer periods, thus leading to a higher crosslink density, the zone size was smaller. Hence it is thought that the larger zone sizes reported by Blundell *et al.* are a reflection of a much lower crosslink density of the host network.

CONCLUSIONS

Sequential interpenetrating networks prepared using poly(dimethylsiloxane) as the host network and polystyrene as the guest network form a phase separated material. Evaluation of the dimensions of the phase separated zones from the analysis of small angle neutron scattering data, shows that these materials are micro-phase separated since their dimensions are *ca.* 150 Å to 600 Å. The dependence of zone size on IPN composition is qualitatively in agreement with the theory of Yeo *et al.*[9] in that a minimum in the curve is obtained. However, the theoretically predicted zone sizes are some four fold greater than those observed, moreover, the marked influence of host network crosslink density predicted is not observed. Experimental observation has shown that it is the crosslink density of the host network which controls the size of the zone and, additionally Yeo *et al*'s. theory shows that is also controls the curvature of its variation with composition, some additional crosslinking of the PDMS network appears to be taking place. However, no unambiguous source for this can be identified as yet. A model dependent analysis of the scattering data has produced evidence for the existence of a preferred separation distance between PSD zones, this was revealed from the existence of some type of structure factor for the zones. Comparison of the experimental scattering with that calculated for a random assembly of hard spheres produced no agreement in the region of low scattering vector wherein the influence of a structure factor would be most important. A broad distribution in zone size has been cited as a possible source for this disparity, but a full analysis for a structure factor requires further small-angle data to be collected at very low values of the scattering vector Q.

ACKNOWLEDGEMENTS

One of us (BM) thanks the Science and Engineering Research Council for the provision of a maintenance grant. Both authors thank J-Sil (Silicones) Ltd for the provision of silicone gums and the staff of the Institut Laue-Langevin, Grenoble, for assistance during SANS measurements.

REFERENCES

1 Olabisi, O., Robeson, I. M. and Shaw, M. T. 'Polymer–Polymer Miscibility', Academic Press, New York, 1979
2 Walsh, D. J., Higgins, J. S. and Maconnachie, A. (Eds.) 'Polymer Blends and Mixtures', NATO. ASI Series E No. 89, Nijhoff, Dordnecht (1985)
3 Rostami, S. and Walsh, D. J. *Macromolecules* 1985, **18**, 1228
4 Warner, M., Higgins, J. S. and Carter, A. J. *Macromolecules* 1983, **16**, 1931
5 Paul, D. R. and Newman, S. 'Polymer Blends Vols. I and II', Academic Press, New York, 1978
6 Klempner, D. and Frisch, K. C. (Eds.) 'Polymer Alloys – Blends, Blocks, Grafts and Interpenetrating Networks', Polymer Science and Technology, Vol. 10, Plenum, New York, 1979
7 Sperling, L. H. 'Interpenetrating Polymer Networks and Related Materials', Plenum, New York, 1981
8 Donatelli, A. A., Sperling, L. H. and Thomas, D. A. *J. Appl. Polym. Sci.* 1977, **21**, 1189
9 Yeo, J. K., Sperling, L. H. and Thomas, D. A. *Polymer* 1983, **24**, 307
10 Michel, J., Hargest, S. C. and Sperling, L. H. *J. Appl. Polym. Sci.* 1981, **26**, 1189
11 Hourston, D. J. and Zia, Y. *J. Appl. Polym. Sci.* 1983, **28**, 3745
12 Widmaier, J. M. and Sperling, L. H. *Macromolecules* 1982, **15**, 625
13 Shilov, V. V., Lipatov, Yu, S., Karbanova, L. V. and Segeeva, L. M. *J. Polym. Sci., Polym. Chem. Edn.* 1979, **17**, 3083
14 Lipatov, Yu. S., Shilov, V. V., Bogdonovitch, V. A., Karbanova, L. V. and Sergeeva, L. M. *Polym. Sci. USSR* 1980, **22**, 1492
15 Blundell, D. J., Longman, G. W., Wignall, G. D. and Bowden, M. J. *Polymer* 1974, **15**, 33
16 Quoted by S. Wu in Chapter 6 of Volume I of ref. 5
17 Guinier, A. and Fournet, G. 'Small Angle Scattering of X-rays', Wiley, New York, (1955)
18 Glatter, O. and Kratky, O. 'Small Angle X-ray Scattering', Academic Press, London, (1982)
19 Kostorz, G. 'Neutron Scattering', Treatise on Materials Science and Technology, Vol. 15, Academic Press, New York, (1979)
20 Richards, R. W. in 'Developments in Polymer Characterisation – 5', (Ed. J. V. Dawkins), to be published by Applied Science
21 Richards, R. W. *Adv. Polym. Sci.* 1985, **64**
22 Zernicke, F. and Prins, J. A. *Z. Phys.* 1927, **41**, 184
23 Ottewill, R. H. in 'Colloidal Dispersion', (Ed. J. W. Goodwin), Royal Society of Chemistry, 1982
24 Debye, P. *Phys. Z.* 1927, **28**, 135
25 Fournet, G. *Acta Crystallogr* 1951, **4**, 293
26 Ashcroft, N. W. and Lekner, *J. Phys. Rev.* 1966, **145**, 83
27 Percus, J. K. and Yevick, G. *J. Phys. Rev.* 1958, **110**, 1

28 Richards, R. W. and Thomason, J. L. *Macromolecules* 1985, **18**, 452
29 Hashimoto, T., Fujimura, M. and Kawai, H. *Macromolecules* 1980, **13**, 1660
30 van Beurten, P. and Vrij, A. *J. Chem. Phys.* 1981, **74**, 2744
31 Debye, P. and Bueche, A. M. *J. Appl. Phys.* 1949, **20**, 518
32 Debye, P., Anderson, H. R. and Brumberger, H. *J. Appl. Phys.* 1957, **28**, 679
33 Kratky, O. *Pure Appl. Chem.* 1966, **12**, 483
34 The divinylbenzene crosslinker was actually a 40% (v/v) solution of divinylbenzene in ethyl benzene
35 Orwoll, R. A. *Rubber Chem. Technol.* 1977, **50**, 451
36 Flory, P. J. and Rehner, J. *J. Chem. Phys.* 1943, **11**, 521
37 Ghosh, R. E., ILL Report No. 81GH29T
38 Porod, G. *Kolloid Z.* 1951, **124**, 83; *ibid.* 1952, **125**, 51, 108
39 Richards, R. W. and Thomason, J. L. *Polymer* 1983, **24**, 1089
40 Wu, S. Chapter 6 in Volume I of ref. 5
41 Helfand, E. and Sapse, A. M. *J. Chem. Phys.* 1975, **62**, 1327
42 McGarey, B. and Richards, R. W., unpublished results
43 Hosemann, R. *Kolloid. Z.* 1950, **117**, 13
44 Cebula, D. J., Ottewill, R. H. and Ralston, J. *J. Chem. Soc. Farad. Trans. I* 1981, **77**, 2585
45 Cebula, D. J., Myers, D. Y. and Ottewill, R. H. *Colloid Polym. Sci.* 1982, **260**, 96
46 Alexander, K., Cebula, D. J., Goodwin, J. W., Ottewill, R. H. and Parentich, A. *Colloid and Surf* 1983, **7**, 233
47 Kinning, D. J. and Thomas, E. L. *Macromolecules* 1984, **17**, 1712
48 Allen, G., Bowden, M. J., Blundell, D. J., Jeffs, G. M., Vyvoda, J. and White, T. *Polymer* 1973, **14**, 604